JOURNAL OF THE AMERICAN WATER RESOURCES ASSOCIATION
Vol. 52, No. 5 AMERICAN WATER RESOURCES ASSOCIATION October 2016

SPATIAL AND TEMPORAL VARIATIONS IN EASTERN U.S. HYDROLOGY: RESPONSES TO GLOBAL CLIMATE VARIABILITY[1]

Dongmei Feng, Edward Beighley, Randall Hughes, and David Kimbro[2]

ABSTRACT: Coastal ecosystems are dependent on terrestrial freshwater export which is affected by both climate trends and natural climate variability. However, the relative role of these factors is not clear. Here, both climate trends and internal climate variabilities at different time scales are related to variations in terrestrial freshwater export into the eastern United States (U.S.) coastal region. For the recent 35-year period, the intensified hydro-meteorological processes (annual precipitation or evapotranspiration) may explain the observed streamflow variability in the northeast. However, in the southeast, streamflow is positively correlated with climate variability induced by the Pacific Ocean conditions (El Nino-Southern Oscillation [ENSO] and Pacific Decadal Oscillation) rather than Atlantic Ocean conditions (Atlantic Multi-decadal Oscillation and North Atlantic Oscillation). The centroid location for volume of terrestrial freshwater export integrated along the eastern U.S. has a positive temporal trend and is negatively correlated with ENSO conditions, suggesting the northward trend in freshwater export to U.S. eastern coast may be disturbed by the natural climate variability, especially ENSO conditions, *i.e.*, the center of freshwater mass moves southward (northward) during El Nino (La Nina) years. The results indicate the spatial and temporal variations in freshwater export from the eastern U.S. are affected by both climate change and inter-annual climate variability during the recent 35-year period (1980-2014).

(KEY TERMS: freshwater export; climate change; natural climate variability; ENSO; coastal.)

Feng, Dongmei, Edward Beighley, Randall Hughes, and David Kimbro, 2016. Spatial and Temporal Variations in Eastern U.S. Hydrology: Responses to Global Climate Variability. *Journal of the American Water Resources Association* (JAWRA) 52(5):1089-1108. DOI: 10.1111/1752-1688.12445

INTRODUCTION

Terrestrial freshwater export into the coastal region is a significant factor affecting the coastal ecosystem. The seasonal and inter-annual variability in freshwater input can affect phytoplankton production, landings, catches, abundance and distribution of some benthic invertebrates and fish species by altering material loading (e.g., nutrients, organic matter, sediments, contaminants and planktonic organisms), physical conditions (e.g., the movement and compression of salt field, stratification, residual circulation), and the hydrodynamic environment (e.g., turbidity, light, chemical, and biological constituents) in estuaries (Quiñones and Montes, 2001; Kimmerer, 2002; Wikner and Andersson, 2012). Thus, to better understand coastal ecosystem, it is important to characterize the temporal and spatial variability in freshwater inputs.

Freshwater input to the coastal region can be strongly affected by climate variations. Production of

[1]Paper No. JAWRA-15-0138-P of the *Journal of the American Water Resources Association* (JAWRA). Received August 20, 2015; accepted May 24, 2016. **Discussions are open until six months from issue publication**.

[2]Graduate Student (Feng) and Associate Professor (Beighley), Civil and Environmental Engineering, and Assistant Professor (Hughes, Kimbro), Marine and Environmental Sciences, Northeastern University, 360 Huntington Ave., Boston, Massachusetts 02115 (E-Mail/Feng: feng.do@husky.neu.edu).

streamflow involves processes of precipitation, soil moisture dynamics, evapotranspiration, and land cover alterations (Poveda *et al.*, 2001; Wooldridge *et al.*, 2001; Karl *et al.*, 2009; Baron *et al.*, 2013). Therefore, it can be affected by factors which have impacts on these meteorological and hydrological processes, such as climatic (e.g., global climate changes, natural climatic variability) and anthropogenic (e.g., land cover changes and water resources policies) processes (Milly *et al.*, 2005; Tootle and Piechota, 2006; Tao *et al.*, 2011; Wang and Hejazi, 2011).

Climate change (as a result of global warming) may impact streamflow by temperature increasing or through changes in the hydro-meteorological cycle (Groisman *et al.*, 2001; Barnett *et al.*, 2005; Tao *et al.*, 2011; Trenberth, 2011). The increase in temperature can lead to a shift of precipitation forms and timing of runoff and then altering streamflow seasonality, especially in snow-dominated regions (Barnett *et al.*, 2005). The increased winter streamflow in the northeast United States (U.S.) is thought to be the result of a shift from snow to rain (Jones *et al.*, 2012), and the earlier onset and increase in spring streamflow in Columbia basin is attributed to earlier snowmelt due to climate change (Dittmer, 2013). Climate change is generally thought to intensify hydrological processes (i.e., precipitation and evapotranspiration) and subsequently impacting streamflow (Barnett *et al.*, 2005; Tao *et al.*, 2011). During the 20th Century, precipitation increased by about 10% over the contiguous U.S. (Karl and Knight, 1998). During the period of 1939-1999, the U.S. national precipitation increased by 7% and streamflow increased by 17%; and the positive trend in heavy precipitation in the eastern U.S. led to increasing frequency of high streamflow (Groisman *et al.*, 2001).

Natural climate variability, mainly driven by ocean conditions, can influence streamflow by altering precipitation through its impacts on atmospheric circulation (Dai, 2013). Several ocean condition indices were defined to investigate internal climate variabilities, including the Pacific Decadal Oscillation (PDO), Atlantic Multi-decadal Oscillation (AMO), North Atlantic Oscillation (NAO), and El Nino-Southern Oscillation (ENSO). Previous studies showed that climate patterns characterized by these indices can affect the U.S. streamflow at inter-decadal (e.g., PDO and AMO), decadal (e.g., NAO), and inter-annual (e.g., ENSO) temporal scales (Tootle *et al.*, 2005). NAO quantifies the normalized sea level pressure difference between the subtropical Azores high and the subpolar Icelandic low, and is a year-round mode of climate variability originating from the Atlantic Ocean that affects the eastern U.S. (Coleman and Budikova, 2013). During high-NAO winters, the extension of Bermuda/Azores high to the northeastern U.S. blocks the invasion of the polar jet stream and the mid-latitude winter storms, which results in the decrease in winter precipitation in northeastern U.S. (Ning and Bradley, 2015) and then alters the streamflow in this region. Coleman and Budikova (2013) found that the NAO, especially the negative phase, can impact the eastern U.S. summer streamflow up to three seasons in advance. During positive NAO years, the southerly wind anomalies induced by the east-west pressure gradient and the blocked invasion of polar jet stream due to extension of Bermuda/Azores high leads to positive temperature anomalies in the northeastern U.S. The AMO is another Atlantic oceanic condition-induced climate variability at a longer time scale compared to NAO. Enfield *et al.* (2001) found that AMO index was positively correlated with rainfall in the northeast and Florida. Ning and Bradley (2014) found that during high-NAO and high-AMO years, the significant positive sea level pressure anomalies and negative relative humidity anomalies occur over the northern part of the northeastern U.S., which leads to decreased precipitation there. ENSO indices, as the indicator of ENSO cycle over the Pacific Ocean, is one of the prominent signals in inter-annual climate variations (McPhaden *et al.*, 2006) and recent studies have also shown that the frequency of extreme El-Nino events may double in the future (Cai *et al.*, 2014). The number of existing studies looking at the effects of ENSO on streamflow in the eastern coastal region is fewer than those focusing on west coast (Cayan *et al.*, 1999; Beighley *et al.*, 2003, 2008). Enfield *et al.* (2001) found that the ENSO conditions were positively correlated with precipitation in Florida and thus contributing to the variability in streamflow in Florida. Ning and Bradley (2014, 2015) found that during strong El Nino winters, more storms generated from the Gulf of Mexico move northward, which leads to increased winter precipitation over the coastal Mid-Atlantic region of the U.S. Kunkel and Angel (1999) found that the below-average frequency of strong cyclone passages in much of the northern U.S. region may explain the below-average snowpack in these areas during strong El Nino winters. Compared to ENSO, PDO is a longer time scale phenomenon across the Pacific Ocean affecting global climate variabilities. During high-PDO years, the 500 hPa geopotential height anomalies block the moisture from the Gulf of Mexico and the Atlantic Ocean entering the northeastern U.S., which results in the decreased winter precipitation (Ning and Bradley, 2014). Recent studies (e.g., Schulte *et al.*, 2016) show that the decadal variability in streamflow in the Mid-Atlantic region of the U.S. is coherent with PDO conditions, and a similar streamflow-ENSO relationship was also identified.

Although human activities (e.g., land cover change and water resources policies) impact streamflow by altering how precipitation is partitioned between evapotranspiration and runoff or how water is stored within a basin, climatic factors can be even more dominant considering they affect both precipitation and evapotranspiration, which are the primary source and loss of streamflow, respectively (Wang and Hejazi, 2011; Zuo *et al.*, 2014). Yang *et al.* (2015) concluded that climate change and variability explained 97.5% variability in streamflow in eastern U.S. during 1901-2010. Therefore, it is reasonable to consider the above-referenced climate factors as primary causes of streamflow variation.

Many prior studies investigated the coupled effects of meteorological factors on streamflow (e.g., Wang and Hejazi, 2011) or only focused on one of them (e.g., Tootle *et al.*, 2005; Tao *et al.*, 2011). However, the relative role of climate change and natural climate fluctuations in regulating streamflow is still not clear. Barros *et al.* (2014) reported that over 80% of streamflow stations in the southeast and Mid-Atlantic U.S. showed no trend during 1980-2010, which may imply that the signal of global warming effects on streamflow may be disturbed by other factors, such as natural climate variabilities. Therefore, investigating relationships between both long-term trends in climate (i.e., climate change) and natural climate variability and streamflow is necessary for understanding how these factors influence streamflow variability and associated effects on coastal ecosystem.

As home to most of the major urban centers in the U.S., the eastern U.S. region draining into the Atlantic Ocean accounts for almost 40% of the U.S. population. High density urban areas can impose great stresses on the aquatic environment. For example, the concentration of polycyclic aromatic hydrocarbons (i.e., a result of burning fossil fuels) in stream sediments in the New England region is 30 times larger than typical background concentrations (Chalmers *et al.*, 2007). Kaushal *et al.* (2013) reported that 62 of 97 selected streams in eastern U.S. have experienced increased alkalization over the past three to six decades. The degraded stream water quality in many parts of the eastern U.S. have been resulting in the coastal ecosystems being more sensitive to temporal and spatial variations to incoming streamflow.

Building on the above, the objective of this study is to investigate the relationships between climate change and natural climate variability with the spatial/temporal variations in terrestrial freshwater export from the eastern U.S. Here, precipitation (P) and evapotranspiration (ET) are used as variables representing climate forcings since they are two key factors involved in climate change affecting streamflow variations. Trenberth (2011) showed that climate change resulted in precipitation trends: decreasing in the subtropics and increasing in mid to high latitudes. Climate change is also believed to lead to increased evapotranspiration trend due to the increased water holding capacity of air (Tao *et al.*, 2011). The higher atmospheric evaporative demand has resulted in increased evaporation in most of the U.S. during the last half century (Peterson *et al.*, 1995; Brutsaert and Parlange, 1998; Brutsaert, 2006). Therefore, trends in P and ET are used here to quantify climate change effects. For natural climate variability, we select four indices, which represent the internal climate oscillations affecting hydrometeorological processes over continental U.S. (Pacific Ocean and Atlantic Ocean) at multiple temporal scales (from multi-decadal to inter-annual), PDO, ENSO, AMO, and NAO. The main work in this article includes: (1) quantifying climate configuration over watersheds in eastern coastal region using data from North America Land Data Assimilation System (NLDAS) (available for the period of 1980-2014); (2) quantifying the spatial and temporal variation in freshwater export along the eastern U.S. for the period 1980-2014 using the available streamflow measurements; and (3) linking the temporal and spatial variations of freshwater export from the eastern U.S. to climate change and the four ocean condition indices. Here, we only focused on the terrain freshwater export and did not cover the estuary region. We suggest that the results of our study combined with improvements in climate change projections and oceanic condition predictions can be used to better understand future freshwater inputs to coastal ecosystem and the corresponding societal benefits, such as aquaculture, fish production, and recreation.

STUDY SITE

In this study, the U.S. eastern region is defined as starting east of the Mississippi River and ending at the U.S./Canadian Border, which includes 21 states: Maine; Vermont; New Hampshire; Massachusetts; New York; Pennsylvania; Connecticut; Rhode Island; New Jersey; Washington, D.C.; Delaware; West Virginia; Maryland; Virginia; North Carolina; Alabama; Mississippi, Georgia; South Carolina; Louisiana; and Florida (Figure 1). Note that, our definition includes portions of both the Gulf and Atlantic coastlines and represents all U.S. watersheds east of the Mississippi River draining into the ocean. The total land area for the study region is approximately 1 million km^2 with over 1,700 watersheds having land areas greater than approximately 10 km^2. Building on existing methods

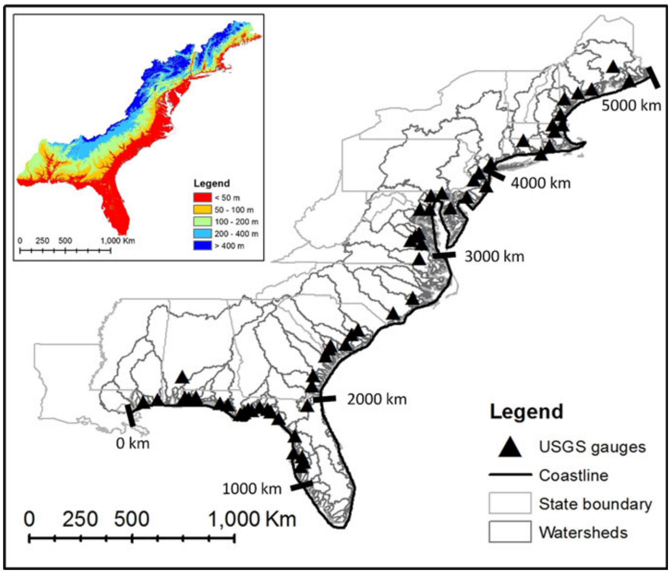

FIGURE 1. Study Region with Watershed Delineations, U.S. Geological Survey (USGS) Streamflow Gauge Locations (triangles) and Reference Coastline with Cumulative Lengths Highlighted; the Small Figure at Left Top Shows the Elevation of the Study Region.

(Beighley and He, 2009; Beighley *et al.*, 2009; Beighley and Gummadi, 2011; Pavelsky *et al.*, 2014), the river network and corresponding sub-watershed and watershed boundaries were determined using ArcGIS Hydrology Tools, gridded flow direction and flow accumulation layers having a horizontal resolution of 3 arc-sec (i.e., roughly 90×90 m^2) from the Hydrosheds dataset (Lehner *et al.*, 2008) available at http://hydrosheds.cr.usgs.gov/, and a threshold area of 10 km^2 to define rivers (i.e., all pixels with flow accumulation values $\geq$10 km^2). There are approximately 3,220 U.S. Geological Survey (USGS) streamflow gauges located in the study region, with a mean drainage area of 1,600 km^2 ranging from 2.6 to 70,500 km^2. There are 54 watersheds that have USGS gauges with daily discharge data at or near their outlets, drain land areas $\geq$260 km^2 (100 mile^2), and have nearly complete data records for the period 1980-2014. The minimum drainage area (260 km^2) and period of record were selected based on the precipitation and evapotranspiration datasets (discussed next) used in this study. The cumulative land area at the outlet of these 54 watersheds is 610,000 km^2 or roughly 60% of the U.S. eastern region (Figure 1) is considered gauged (Moglen and Beighley, 2000; Pavelsky *et al.*, 2014) in our study. For this study, watershed outlets were defined as the last pixel along each main river prior to the coastline (i.e., edge of the Hydrosheds dataset). To assess the derived network, drainage areas at each gauge location were determined and compared with the values reported by the USGS. The overall agreement is good with an average absolute error of only 5.4%. Although the gauges are not located at the exact watershed outlets as defined here, the mean and median area ratios are 76 and 79%, respectively (i.e., gages capture much of the overall watershed area). To estimate watershed streamflow, gage values were scaled using the watershed outlet to gage location area ratio.

DATA

The central data used in this study are streamflow (Q), precipitation (P), evapotranspiration (ET), temperature (T), and the climatic indices including NAO, AMO, ENSO, and PDO. Annual streamflow data were obtained from the USGS (http://waterdata.usgs.gov/nwis/sw). For P and T, we used monthly data from Phase 2 of the North American Land Data Assimilation System (NLDAS-2), which has a spatial resolution of $0.125° \times 0.125°$ (roughly 12.5×12.5 km^2) with measurements starting in 1979 (Mitchell *et al.*, 2004). For ET, we used monthly values derived from the output of NLDAS VIC Land Surface Model; L4 Monthly Climatology (Xia *et al.*, 2012). The AMO is defined as the detrended Sea Surface Temperature (SST) anomalies over North Atlantic basin (0 to 70°N). Here, we used an unsmoothed version of monthly AMO index. For the ENSO conditions, we used the Oceanic Niño Index [three month running mean of ERSST.v3b SST anomalies (Xue *et al.*, 2003)] in the Niño 3.4 region (i.e., a box spanning 5°N to 5°S latitude and 120°W to 170°W longitude). PDO is derived as the leading principal component of monthly SST anomalies in North Pacific Ocean (poleward of 20°N). Both NAO and ENSO indices were obtained from the National Center for Environmental Prediction's Climate Prediction Center (http://www.cpc.ncep.noaa.gov/). The AMO data are obtained from the National Oceanic and Atmospheric Administration's Earth System Research Laboratory's Physical Science Division (http://www.esrl.noaa.gov/psd/). The PDO index is from the Joint Institute for the Study of Atmosphere and Ocean at the University of Washington (http://research.jisao.washington.edu/pdo/).

METHODS

Trend Analysis

Generally, the methods for trend analysis are classified into two categories: parametric methods (e.g., linear regression of random response variables on time or "space" for spatial trend analysis) and nonparametric methods (e.g., Mann-Kendall, MK, trend test (Mann, 1945; Kendall, 1975) and Spearman's rho (SR) test (Lehmann, 1975)) on random response variables. Nonparametric tests, compared with parametric methods, require a relaxed form of distributional types, that is, they do not need the data to be normally distributed but only serially independent and identically distributed (i.e., similar variance over time) (Helsel and Hirsch, 1992; Poona and Storch, 1995; Yue *et al.*, 2002; Gocic and Trajkovic, 2013). The advantages of nonparametric procedures are fewer assumptions on the underlying quantity distributions, less sensitive to a small percent of outliers, invariant to power transformation (e.g., MK tests give the same *p*-values when applied to the original time series and the log-transformed series), and simplicity in application (Helsel and Hirsch, 1992; Shadmani *et al.*, 2012). Therefore, in climatological and hydrological applications where the normality and independence of observations are often not satisfied, nonparametric trend test methods, such as Mann-Kendall (Lins and Slack, 1999; Zhang *et al.*, 2001, 2006; Kahya and Kalaycı, 2004; Wu *et al.*, 2008; Birsan *et al.*, 2014) and Spearman's rank correlation coefficient (El-Shaarawi *et al.*, 1983; Hipel and McLeod, 1994; Yue *et al.*, 2002; Khaliq *et al.*, 2009) are preferred. Yue *et al.* (2002) showed that the MK and SR have similar power for trend analysis in both normally distributed and highly skewed time series. Therefore, in this study, both Mann-Kendall and Spearman's rank correlation coefficient tests are used. When applying these methods, serial correlation needs to be considered due to its contribution to evidence for null hypothesis rejection, which may be misleading during trend analysis. However, when collected with sufficiently large gaps, such as one year, or when seasonal or monthly data are aggregated into annual summary values, these series have minimal serial dependence and trend tests can be carried out "in straightforward fashion" (Hirsch and Slack, 1984; Poona and Storch, 1995). Considering annual data are analyzed in this work, no serial correlation tests or pre-whitening procedures are carried out before applying trend test methods.

In most trend tests, the level of significance can alter the results. Commonly used level of significance values are 1% (Beighley and Moglen, 2002; Birsan *et al.*, 2014), 5% (Zhang *et al.*, 2006; Wu *et al.*, 2008; Ramadan *et al.*, 2012), and 10% (Zhang *et al.*, 2001). Here, the significance level is used to describe the probability of type I error, that is, the probability of rejecting the null hypothesis when it is true. The null hypothesis in this paper is: samples are independent and identically distributed (i.e., there is no temporal trend in selected samples). A significant trend at a 5% significance level means that the probability of falsely identifying the trend is 5%. However, as the significance level decreases, more evidence is required to reject the null hypothesis, and it is more likely to accept the null hypothesis when in fact it is false and should be rejected (i.e., make a Type II error). Given the importance and challenge (e.g., tradeoff between Type I *vs.* II errors) of selecting the level of significance, we explore 1, 5, and 10% levels.

Test of Correlation with Oceanic Conditions

To quantify the effects of ocean conditions on P, T, ET and Q, the Kendall Tau and Spearman rank correlation methods are used in a correlation analysis. As with the trend analysis, we use level of significance values of 1, 5, and 10%. This analysis is implemented at annual temporal resolution. Annual streamflow is collected from USGS station records, and annual P, ET and T data are obtained by summing NLDAS-2 monthly precipitation and NLDAS VIC land surface model L4 monthly ET data, and averaging monthly temperature data. All of these data are analyzed using water years (e.g., water year 2011 is October 1, 2010 to September 30, 2011). Here, we determine the annual climate indices by averaging the monthly values over the water year. For the monthly analysis, the correlations between monthly Q, ET, P, T, and climate indices for 1 to 12 months prior were analyzed to determine the relevant lag period for each ocean condition index. For example, correlation between JAN 2010 streamflow and ENSO indices from JAN 2009 to DEC 2009 were determined for each watershed, then the ratio of watersheds area showing significant correlation with the total area is calculated for each lag time and the largest ratio of significant correlation was selected to represent the optimal lag time between natural climate conditions and the resulting hydrologic conditions.

Spatial Analysis

To define the spatial location of each watershed in the study region, a length value was assigned to each watershed's outlet location. The length values range from zero at the starting point located at the southwest corner of the study region to roughly 5,000 km at the ending point in the northeast corner of the study region, where length is measured along the coastline (see Figure 1). Thus, each watershed is assigned a length value that represents its outlet location along the coastline. The volumetric centroid location of Q, P, and ET along the coastline is utilized to quantify the spatial distribution and variation in

Q, P, and ET as related to the eastern U.S. coastal region. We favor volumetric centroid location as a feature to quantify the spatial variation in hydrologic variables for a few reasons. (1) It integrates the spatial distribution of hydrologic variables into one index, which is easier to describe the dynamics of the spatial variation in these hydrologic variables, considering the spatial heterogeneity of hydrological processes over the eastern U.S.; (2) it can be used to calculate the trend and correlation of P, ET, and Q with the climatic indices for the entire study region, which provides a new perspective to look at the dynamics of and effects of climatic factors on hydrologic cycle; and (3) spatial variations in dynamic hydrologic variables can be amplified when considering the volumetric centroid location, for example, a small increase in Q in the northeast and a slight decreasing in Q in the southeast, which may be statistically insignificant, can make a significant change in the volumetric centroid location, which is helpful to identify its relationship with the climatic factors.

For a given quantity, the centroid location is determined by:

$$l_c = \frac{\sum_1^n q_i \times l_i}{\sum_1^n q_i}, \tag{1}$$

where l_c is the centroid location (km), q_i is freshwater export (or watershed averaged P and ET) from watershed i (km^3), l_i is the outlet location of watershed i measured along the coastline (km), and n is the number of watersheds. To determine watershed export and to convert streamflow to runoff, we used the drainage area of each gauge to determine runoff depth and approximated that value for the entire watershed area.

RESULTS AND DISCUSSION

The average annual rainfall (Figure 2a) over the study region for the period of 1980-2014 can be characterized into three categories: <1,160, 1,160-1,290, and >1,290 mm/yr. Note that, Figures 2a, 2b, 2c, 2d legends correspond to the low, average, and high values, where the average value range is defined by the annual mean ± 1/2, 1/3, 1 and 1/2 standard deviation, respectively, and the ranges of categories are selected to best represent spatial pattern of P, ET and Q over the study region. The Gulf Coast region experienced the highest rainfall and the Mid-Atlantic region had the lowest precipitation. The average annual ET (Figure 2b) had an obvious spatial pattern: high ET in the south, and low ET in the north. The mean of annual streamflow (Figure 2c) increased from south to north, except for the Gulf of Mexico region. This pattern can be found during the whole study period. Figure 3 shows the distribution of annual streamflow in a typical year (e.g., in WY 2013 annual runoff is 438 mm and mean annual runoff of the study period is 424 mm), the wettest year (WY 1998), and the driest year (WY 2002). In general, annual streamflow decreased with distance from 0 to 1,500 km (which includes the region from the Gulf Coast to the west coast of Florida) and then increased from 1,500 km (southeastern corner of Florida) to 5,000 km (northeastern U.S.). Most (51/54) of the gauged watersheds follow this pattern except a small watershed (USGS gauge no. 02359500) located along the Gulf Coast which tends to produce more runoff and two other watersheds (USGS gauge no. 02171500 and 01403060) that produce less runoff. This pattern can be explained by the different spatial distribution of P and ET: moderately high rainfall and low ET results in high streamflow in the northern region, while moderate rainfall and high ET produces low streamflow in the South-Atlantic region. The average runoff coefficient Q/P ratio (Figure 2d) had a similar spatial pattern to streamflow. The highest Q/P (>0.5) was located in the north (mainly New England region) and the lowest Q/P (<0.25) was located at the middle to the southeast regions. The Q/P ratio likely mimics the Q pattern due to nonlinear rainfall-runoff processes (i.e., small changes in P can results in large changes in Q) and the relative magnitude in the spatial variations in P and Q. For example, the standard deviation in annual P throughout the domain is roughly 130 mm with a domain mean of 1,200 mm (11%) while the standard deviation in annual Q throughout the domain is roughly 235 mm with a domain mean of 450 mm (52%).

It is also important to note that the ET values used in this study are model output, P and T are reanalysis data products, and Q values are based on point measurements from streamflow individual stations. As a check on these datasets, we compared monthly water balance (Q = P − ET) for each watershed. The mean ratio of measured to calculated annual runoff, Q/(P − ET), is approximately 70%. Although not a perfect agreement, the standard deviation of the annual ratios is <10% suggesting that the ratio is relatively consistent from year to year (i.e., consistent bias in P and/or ET). Thus, while P may be high or ET may be low, it appears that their bias is consistent from year to year. In this study, we analyzed each time series separately, which minimizes potential impacts of consistent bias in ET or P. However, future research efforts should specifically explore additional P datasets and ET estimation methods for the region.

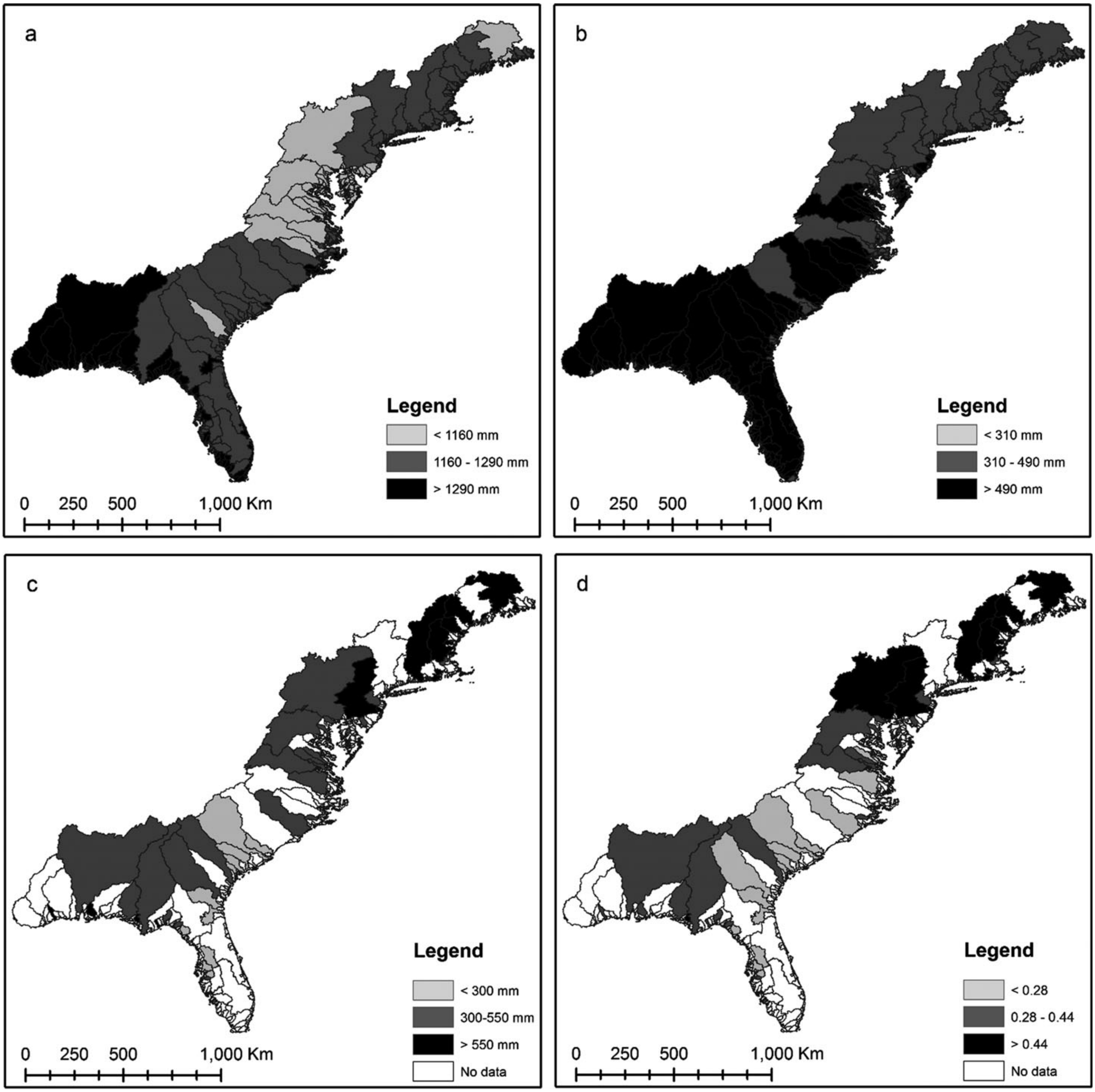

FIGURE 2. Average Annual (a) Precipitation, (b) Evapotranspiration, (c) Streamflow, and (d) Runoff Ratio during Water Years 1980-2014.

Impact of Climate Change on Streamflow

The trend analysis results are shown in Table 1 and Figure 4 and for the sake of space conservation, only results at 5% significance level are discussed here. The increase in temperature was identified throughout eastern U.S. except for the southeast region of Florida. More than 80% area of the eastern U.S. experienced a warming trend. A similar result was also found by Ficklin *et al.* (2015). About 25% of the study region, mainly located in the northern part, shows an increasing trend in ET and the rest shows no significant trend in ET except several small watersheds in west Florida showing a negative trend. Previous studies about the changes in evapotranspiration during the past decades are contradictory: some found that there is an increasing trend in ET during the past five to six decades and they

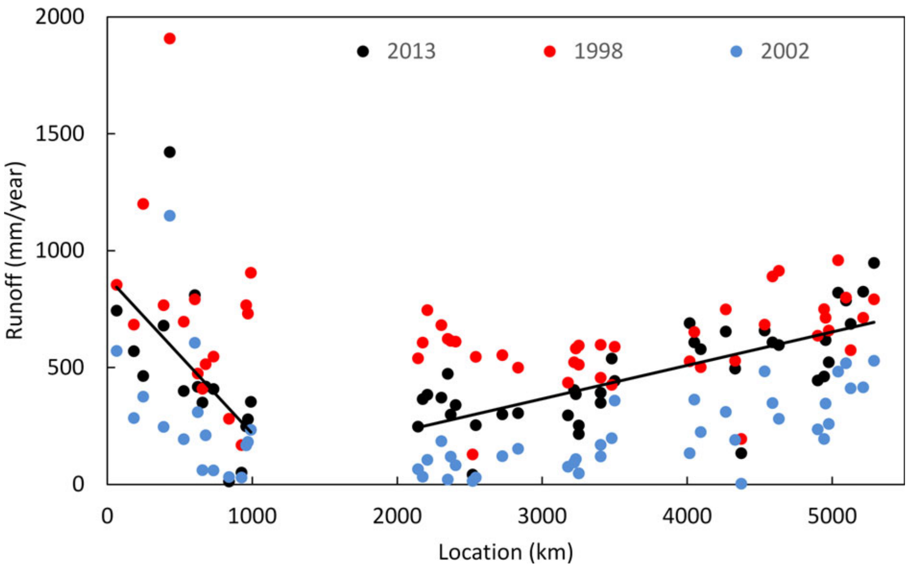

FIGURE 3. Annual Discharge from Watersheds Draining Eastern United States along the Coastline in Water Years 2013 (mean), 1998 (wettest), and 2002 (driest).

contributed this pattern to the intensified hydrologic cycle induced by global warming (Brutsaert and Parlange, 1998; Brutsaert, 2006; Vicente-Serrano *et al.*, 2014; Ficklin *et al.*, 2015); while others showed that little changes in potential ET were found (Sheffield *et al.*, 2012). The main reason for this difference is the interpretations of ET measurement and methods used for calculating potential ET. The results in our work show that the trend in ET is region-specific. The northern region, showing an increasing ET, also experienced an increasing precipitation, although over a smaller area (6% of total study region area) (Figure 4). The increasing precipitation, which can increase surface runoff, soil moisture, and specific humidity, may be one reason for the increasing ET trend. In the southern region, there is no significant trend in ET as well as P. These findings may imply that the response of ET to climate changes may be region-specific and air temperature is not the only factor affecting ET changes (Ficklin *et al.*, 2015).

An increasing trend in P was found in 6% of the study area located only in the north and no significant trend in P was found in the Mid-Atlantic or southern regions. This is consistent with previous studies (Horton *et al.*, 2011; Trenberth, 2011; Seager *et al.*, 2012; Pederson *et al.*, 2013) which found the increasing trend in P in the northeastern U.S. Trenberth (2011) stated that the increasing precipitation trend in mid to high latitudes results from climate change. Horton *et al.* (2011) projected that mean precipitation in New York City increases by 5-10% to 2080s under the background of climate change based on the output of 16 global climate models. However, Seager *et al.* (2012) concluded that the pluvial conditions in the northeastern U.S. since 1980 are neither forced by anthropogenic climate change nor by the oceanic conditions. The investigation about the cause of the trend in P is beyond the scope of this work, but the results in our work showing region-specific trend in P may imply that the mechanisms affecting changes in P are complex and the effects of climate change on P may be obscured by other factors, such as the natural climatic variability.

As an integrated measure of P and ET changes, streamflow shows an increasing trend in 7% of the study area, which is also located at the northeastern region. This is consistent with previous studies, for example, Wang and Hejazi (2011) found that climate changes tended to increase streamflow in the northeast. The positive streamflow trend occurs in area experiencing both increasing P and ET. Although increasing ET could mitigate any increases in P, the increasing Q implies that the effects of ET in regulating the variability in streamflow are small compared to precipitation. A negative trend in Q was identified in a smaller area (4%) in the South-Atlantic and Florida regions. However, in these regions, no increasing precipitation or decreasing ET was found; therefore, the negative trend in streamflow may be due to other factors, such as human activities. Wang and Hejazi (2011) found that there is a decreasing trend in mean annual streamflow in Florida and both climate variations and direct human activities decreased the mean annual streamflow in the Florida region for the period of 1948-2003. Barros *et al.* (2014) attributed the decreasing trend in annual peak streamflow in Florida to karst processes and sink-hole activity. We did not consider the effects of potential land use and land

TABLE 1. Trend Test Results for Annual Mean Temperature (T) and Annual Precipitation (P), Evapotranspiration (ET), Streamflow (Q) Averaged Watersheds Draining the Eastern United States for Water Years 1980-2014.

Trend Analysis		Spearman			Mann Kendall		
		Significant ($p \leq 0.05$)		Not Significant ($p > 0.05$)	Significant ($p \leq 0.05$)		Not Significant ($p > 0.05$)
		(–)	(+)		(–)	(+)	
Q	Count	6	4	44	6	3	45
	% in area	4	7	89	4	2	94
P	Count	87	68	1,550	82	59	1,564
	% in area	0.5	6.4	93.2	0.4	3.1	96.4
T	Count	584	845	277	577	842	287
	% in area	2	81	17	2	80	18
ET	Count	177	292	828	178	262	857
	% in area	2	26	71	2	23	75

cover changes on streamflow in this work. Even though land use and land cover changes exert less impacts on regulating streamflow compared to climatic processes (e.g., precipitation and ET), a further investigation in future work may help explain the streamflow variations.

A trend analysis was also performed for the annual P, ET and Q volume summed over the study region. For consistency, only watersheds with streamflow records are considered. Total volume of P, ET and Q (m/yr) was determined by summing the volume from each watershed (m^3/yr) and dividing by total drained area of those watersheds (km^2). The results (not shown in figures or tables) show that there is no statistically significant temporal trend in the total volume of P, ET and Q during water years 1980-2014. In spite of the positive trend in P, ET, and Q in the northeast, the total volume of P, ET, and Q over the eastern U.S. did not show any significant trend, which indicates that the temporal variability in P, ET, and Q in the south of the study region counteracted the increasing trends in the northeast (i.e., near zero net change over the entire region).

Correlation with Natural Climate Variability

The analysis results for the correlation of P, ET, Q, and T with natural climate variability indices (at 5% significance level) are illustrated in Figure 5 and Tables 2-5. For temperature, from Figure 5, we can find that about 7% of study area, located in Florida, showed significant correlation between NAO and mean annual T. Previous studies (Kenyon and Hegerl, 2008) show that the effects of NAO on winter temperature in the U.S. are dipole, that is, the positive NAO phase brings more cold days in the New England region, which result in more warm days in the south part. The absence of significant correlation in most of the study region may be because NAO is a mainly winter time phenomenon, and the annual analysis may erase the effects of NAO on temperature over the study region. Recent studies (Li *et al.*, 2011, 2012, 2013; Ortegren *et al.*, 2014) showed that the westward movement of the Bermuda-Azores high in the recent three decades regulated the summer moisture transport over the southeastern U.S. and thus affecting the climate there, which may be contributing, if any, to the significant correlation between T and NAO there. PDO and AMO showed a significant correlation with T in 89% and 79% area, respectively. By further examining the PDO and AMO, we find that during the study period 1980-2014, PDO experienced a transition from a warm phase to a cool phase, and opposite for AMO, from cool phase to warm phase. The phase transitions of PDO and AMO led to a negative and positive temporal trend, respectively, for the study period, which may result in spurious significant correlations between PDO/AMO and temperature over the eastern U.S. There is no significant correlation between ENSO and mean annual T in the eastern U.S.

For precipitation, there is no significant correlation with NAO, PDO, or AMO. However, 52% of the area, located in the southern portion of the study region, showed significant correlation between ENSO and P. Sea surface temperature anomalies over the Pacific Ocean have a strong influence on precipitation in the U.S. due to impacts on atmospheric circulation (Dai, 2013). ENSO events can initiate particular circulation anomalies in the extra tropical atmosphere and thus affect the strength and path of jet streams which determine the distribution of precipitation over the U.S. (Hu and Feng, 2012; Yu and Zou, 2013). During El Nino years, the trough of the jet stream shifts east of its normal position, which brings more tropical moisture eastward to the southern U.S. and increases precipitation. Moreover, the ENSO events also impact the number and intensity of tropical

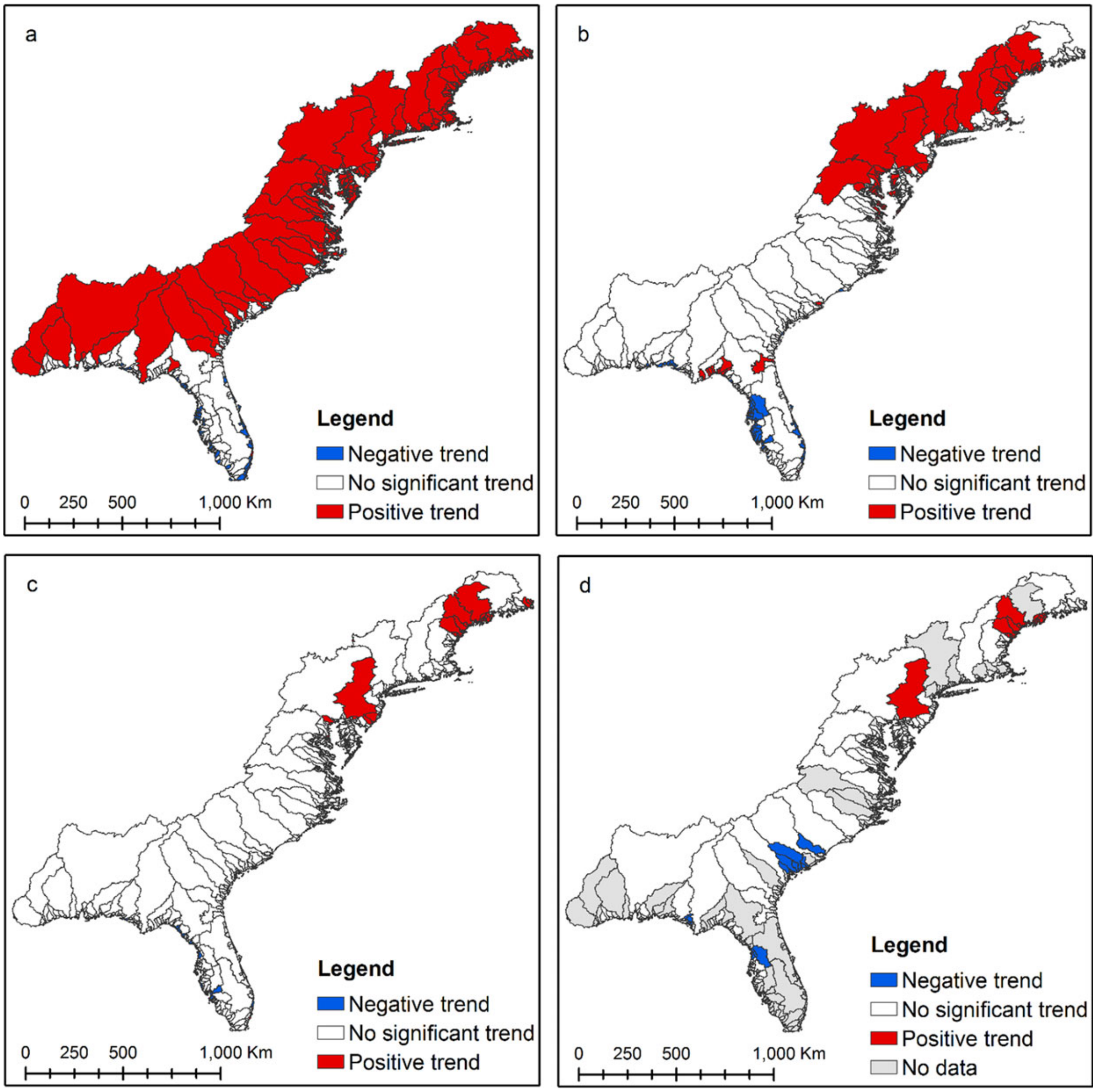

FIGURE 4. Trend in Annual (a) Temperature, (b) Evapotranspiration, (c) Precipitation, and (d) Streamflow from Gauged Watersheds Located along the Eastern United States for Water Years 1980-2014.

cyclone activities over the North Pacific and North Atlantic oceans. During El Nino years, both the number and intensity of tropical cyclones over eastern North Pacific increase, which may also make a contribution to the increase in precipitation in the southeast of U.S. (Larson *et al.*, 2005). Further examination of the relation between monthly rainfall and ENSO indices revealed that the significant annual rainfall-ENSO relationship in the South-Atlantic mainly resulted from the significant correlation between October, November, and December monthly rainfall and ENSO conditions four months prior (Table 6). This result is consistent with previous studies which indicate that ENSO impacts on precipitation are strongest in boreal winter compared to other seasons (e.g., Hu and Feng, 2012). During El Nino (La Nina) winters, there are above-average (below-average) frequency of strong cyclone activities compared to normal years in the southeastern U.S., which lead to higher (lower) precipitation (Kunkel and Angel, 1999). Thompson *et al.* (2013) found that during El Nino years, there is higher frequency of winter storms in the Gulf of Mexico and the southeast of U.S. than in La Nina years.

For ET, there is no significant correlation between mean annual ET over eastern U.S. and NAO. About 12% of the area, located in the northern part, showed significant correlation between ET

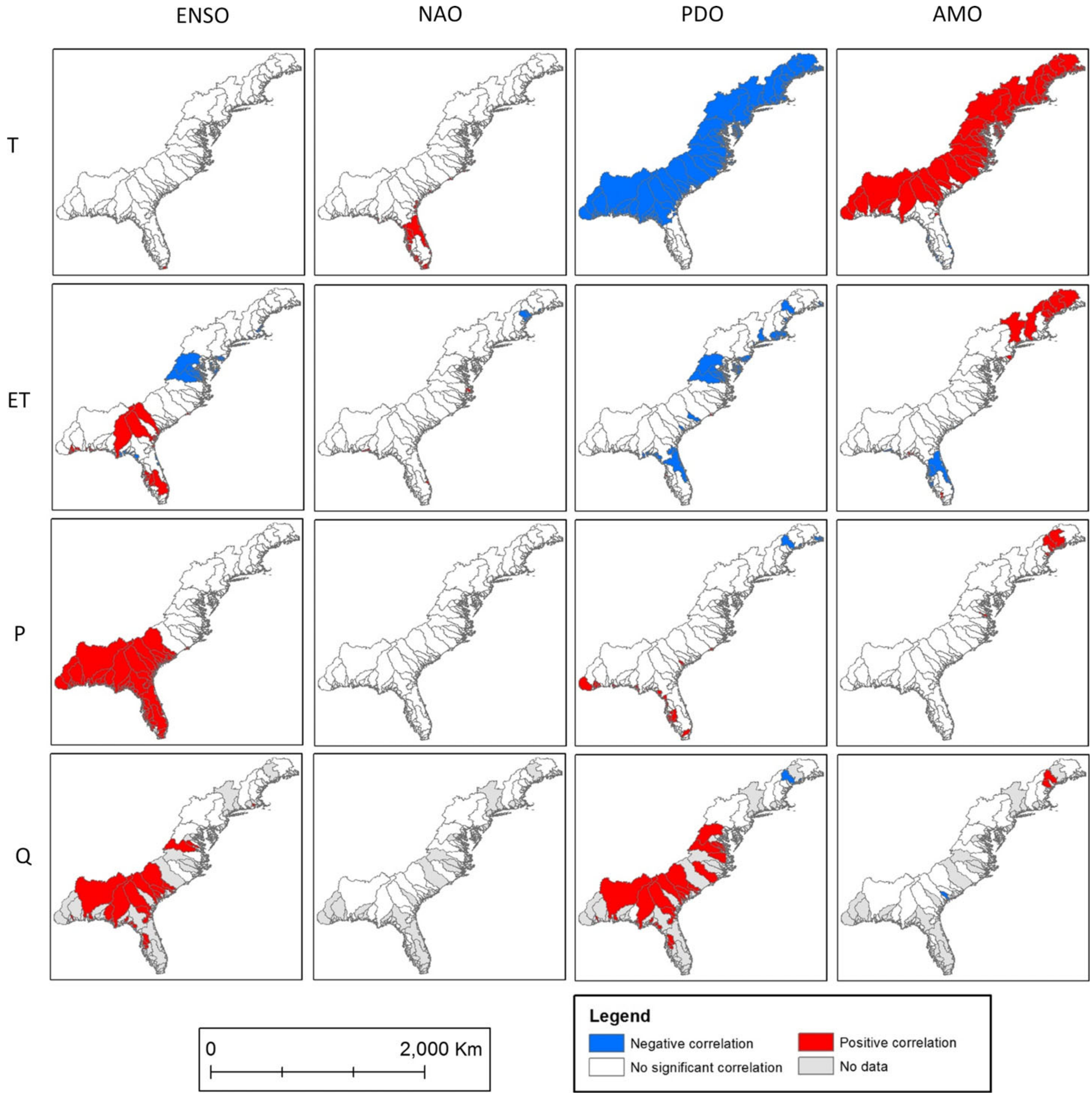

FIGURE 5. Correlation between Annual Temperature (T), Precipitation (P), Evapotranspiration (ET), and Streamflow (Q) Integrated from Gauged Watersheds along the Eastern United States *vs.* North Atlantic Oscillation (NAO), El Nino-Southern Oscillation (ENSO), Pacific Decadal Oscillation (PDO), and Atlantic Multi-decadal Oscillation (AMO) Conditions for Water Years 1980-2014.

and PDO and AMO. Similar to the relationship with T, the significant ET-PDO and ET-AMO correlation in the north may be due to the spurious trend resulting from the phase transition of PDO and AMO. For ENSO, 15% of the area, located in the south, showed a significant positive correlation between ET and ENSO; and 8% of the area, located in the Mid-Atlantic region, showed negative correlation between ET and ENSO. By comparing P and ET, we can find the area showing significant positive ET-ENSO correlation is also showing significant positive P-ENSO correlation, which may imply that ENSO conditions impact ET by altering water availability as compared to available

TABLE 2. Correlation with El Nino-Southern Oscillation in Annual Mean Temperature (T) and Annual Precipitation (P), Evapotranspiration (ET), Streamflow (Q) Averaged from Watersheds Draining the Eastern United States for Water Years 1980-2014.

Correlation Analysis		Spearman			Kendall		
		Significant ($p \leq 0.05$)		Not Significant ($p > 0.05$)	Significant ($p \leq 0.05$)		Not Significant ($p > 0.05$)
		(+)	(−)		(+)	(−)	
Q	Count	0	27	27	0	29	25
	% in area	0	58	42	0	60	40
P	Count	0	470	1,235	0	463	1,242
	% in area	0.0	51.9	48.1	0.0	51.8	48.2
T	Count	0	1	1,705	0	2	1,704
	% in area	0	0	100	0	0	100
ET	Count	288	116	893	290	116	891
	% in area	8	15	76	8	15	76

TABLE 3. Correlation with North Atlantic Oscillation in Annual Mean Temperature (T) and Annual Precipitation (P), Evapotranspiration (ET), Streamflow (Q) Averaged from Watersheds Draining the Eastern United States for Water Years 1980-2014.

Correlation Analysis		Spearman			Kendall		
		Significant ($p \leq 0.05$)		Not Significant ($p > 0.05$)	Significant ($p \leq 0.05$)		Not Significant ($p > 0.05$)
		(+)	(−)		(+)	(−)	
Q	Count	0	0	54	0	0	54
	% in area	0	0	100	0	0	100
P	Count	0	1	1,704	0	1	1,704
	% in area	0.0	0.0	100.0	0.0	0.0	100.0
T	Count	9	572	1,125	16	525	1,165
	% in area	0	7	93	0	7	93
ET	Count	23	62	1,212	14	71	1,212
	% in area	1	0	98	1	1	98

energy through intensifying precipitation in the southeastern U.S.

For streamflow, there is no significant correlation between Q and NAO or AMO. Previous studies found that NAO influences the intra-seasonal variations of streamflow in the northeastern U.S. (Coleman and Budikova, 2013). However, in the present work, we did not find a significant correlation between NAO and Q, one possible reason is that here we focus on the annual temporal scale and the intra-seasonal variability in Q may be missed when monthly data were integrated into annual time series. About 60% of the area, located in the Mid-Atlantic and South Atlantic-Gulf regions, show significant correlation between Q and ENSO. Compared to ENSO-P and ENSO-ET relationship, significant ENSO-Q relationships are found for a larger area: roughly 15-50% of the area for ET and P, increasing to about 60% of the area for Q. The spatially expanded ENSO impacts on Q compared to those on P and ET, are also noted by other previous studies (Poveda *et al.*, 2001; Wooldridge *et al.*, 2001; Karl *et al.*, 2009; Baron *et al.*, 2013). This may be the case because Q integrates both P and ET processes which can make it more sensitive to ENSO conditions. About 60% of the area shows significant correlation between Q and PDO, and the spatial distribution is almost the same with that of ENSO. The similar ENSO-Q and PDO-Q relationships were also identified by other researchers, Schulte *et al.* (2016), for example, who found similar patterns of ENSO and PDO relationship with streamflow in Mid-Atlantic region of the U.S. The similarity between ENSO-Q and PDO-Q relationships can be explained by the linkage between ENSO and PDO. Previous studies (Newman *et al.*, 2003) showed that ENSO is a leading mode of PDO index by a few months. Schulte *et al.* (2016) explained the similar Q-ENSO and Q-PDO relationship by using the "atmospheric bridge" theory proposed by Alexander *et al.* (2002). They suggest that the anomalously strong Aleutian low during El Nino phases, an essential component of atmospheric bridge, can result in negative sea surface temperature in central North Pacific which leads to a positive mode of PDO.

TABLE 4. Correlation with Pacific Decadal Oscillation in Annual Mean Temperature (T) and Annual Precipitation (P), Evapotranspiration (ET), Streamflow (Q) Averaged from Watersheds Draining the Eastern United States for Water Years 1980-2014.

Correlation Analysis		Spearman			Kendall		
		Significant ($p \leq 0.05$)		Not Significant ($p > 0.05$)	Significant ($p \leq 0.05$)		Not Significant ($p > 0.05$)
		(+)	(−)		(+)	(−)	
Q	Count	2	28	24	2	27	25
	% in area	2	67	32	2	60	38
P	Count	24	249	1,432	29	253	1,423
	% in area	1.2	4.5	94.3	2.8	4.9	92.3
T	Count	901	2	803	891	2	813
	% in area	88	0	12	89	0	11
ET	Count	416	35	846	418	37	842
	% in area	15	0	84	18	0	82

TABLE 5. Correlation with Atlantic Multi-decadal Oscillation in Annual Mean Temperature (T) and Annual Precipitation (P), Evapotranspiration (ET), Streamflow (Q) Averaged from Watersheds Draining the Eastern United States for Water Years 1980-2014.

Correlation Analysis		Spearman			Kendall		
		Significant ($p \leq 0.05$)		Not Significant ($p > 0.05$)	Significant ($p \leq 0.05$)		Not Significant ($p > 0.05$)
		(+)	(−)		(+)	(−)	
Q	Count	1	2	51	0	0	54
	% in area	1	2	97	0	0	100
P	Count	13	74	1,618	13	64	1,628
	% in area	0.0	3.0	97.0	0.0	1.5	98.5
T	Count	604	856	246	596	850	260
	% in area	2	80	18	2	79	19
ET	Count	155	57	1,085	144	60	1,093
	% in area	4	12	84	4	7	89

TABLE 6. Fractions of Watershed Area Showing Significant Correlation between Monthly Precipitation (P), Evapotranspiration (ET), Streamflow (Q) and El Nino-Southern Oscillation Index Four Months Prior.

	Month											
	January	February	March	April	May	June	July	August	September	October	November	December
P	0.157	0.092	0.004	0.053	0.104	0.264	0.021	0.006	0.012	0.451	0.452	0.339
ET	0.000	0.710	0.024	0.050	0.095	0.252	0.170	0.269	0.016	0.104	0.016	0.067
Q	0.557	0.469	0.087	0.015	0.425	0.520	0.529	0.100	0.092	0.323	0.703	0.445

The correlation analysis was also performed for the annual P, ET, and Q volume summed over gaged watersheds. The results show that there is no significant correlation between NAO/AMO and the total volume of P, ET, and Q during water years 1980-2014, ENSO shows significant positive correlation with the volume of P ($p < 5\%$) and Q ($p < 1\%$), and PDO shows significant positive correlation with the volume of Q ($p < 5\%$) (Table 7). As discussed above, the positive correlation between ENSO and the volume of P and Q mainly results from the increase (decrease) of P and Q in the southern region during El Nino (La Nina) years.

Spatial Variation

The inter-annual variability for the spatial distribution of P, ET and Q is characterized by the centroid location (volumetric center) calculated using Equation (1), and the results are shown in Figure 6. Over the entire period, the centroid location for P shifts between 2,061 and 2,567 km with a mean at 2,242 km. For ET, a smaller variation in centroid location is found: the centroids shift between 2,680 and 2,829 km with a mean at 2,755 km for all years. The centroids of Q centers averagely at 2,800 km with a range from 2,382 to 3,418 km.

TABLE 7. Correlation with El Nino-Southern Oscillation (ENSO)/ Pacific Decadal Oscillation (PDO) in Annual Precipitation (P), Evapotranspiration (ET), and Streamflow (Q) from Gauged Watersheds Located along the Eastern United States for Water Years 1980-2014; Bold *p*-Values Indicate a Significant Trend at 5% Level of Significance.

	ENSO				PDO			
	Spearman		Mann-Kendall		Spearman		Kendall	
	rho	*p*	tau	*p*	rho	*p*	tau	*p*
Q	0.460	**0.005**	0.325	**0.006**	0.374	**0.027**	0.266	**0.025**
P	0.365	**0.031**	0.254	**0.032**	0.186	0.284	0.128	0.280
ET	0.076	0.666	0.056	0.639	−0.210	0.225	−0.145	0.222

We also examined the temporal trend in the centroid location of P, ET and Q based on Spearman and MK tests. The results are shown in Table 8 and Figure 6. Both P and Q showed significant temporal trend ($p < 15\%$) in their spatial distributions during the period 1980-2014. ET exhibited more significant temporal trend ($p < 2\%$) in its centroid location. All quantities showed positive trends, which suggests that the center of mass for P, Q, and ET from the eastern U.S. is tending to move toward north. The centroid locations of Q, P, and ET move toward north by 400, 130, and 50 km, respectively, during the study period based on the linear regressions shown in Figure 6. This temporal trend is likely attributable to

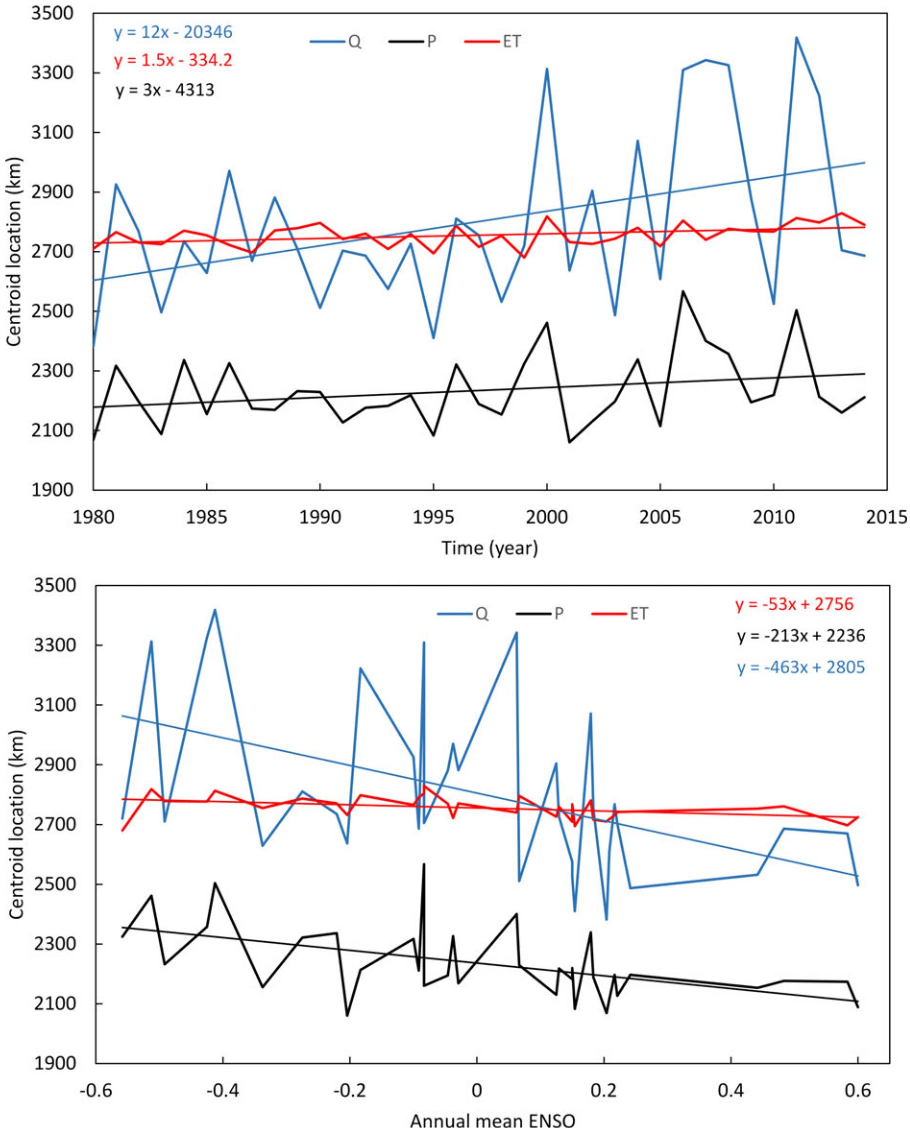

FIGURE 6. The Centroid Locations of Annual Precipitation (P), Evapotranspiration (ET), and Streamflow (Q) from Gauged Watersheds along the Eastern United States for Water Years 1980-2014 (top) and Their Relation to El Nino-Southern Oscillation (ENSO) Index (bottom).

climate change. As discussed above, increasing temporal trends in ET, P and Q in the north may lead to the northward trend of centroid locations over the past 35 years. In addition, both duration and peak intensity of the tropical cyclones in the North Atlantic increased during the past two to three decades (Emanuel, 2005; Klotzbach, 2006), and the global climate model projections also indicate that the anthropogenic climate change will cause higher frequency of strong tropical cyclones (Knutson *et al.*, 2010; Emanuel, 2015). Although the trends of historical tropical cyclones are controversial due to the availability and quality of the records of tropical cyclones (Landsea *et al.*, 2006) and the projections from different modelling studies show variations (Knutson *et al.*, 2010; Vecchi *et al.*, 2013), the changes in tropical cyclones along with changes in precipitation from these storms may also be a possible reason inducing the trends in the centroid locations of P and Q. Compared to P and Q, the rate of northward movement of ET center is relatively small, suggesting a strong connection to available solar radiation, which is largely independent of regional or global climate variability (i.e., radiation is highly dependent on latitude and time of year), and a tendency for ET to be energy limited rather than water limited.

The correlation between the centroid locations of P, ET and Q and the four climate indices shows that the centroid locations for P, ET and Q are significantly correlated with ENSO ($p < 5‰$) and PDO ($p < 5\%$ except for P) (Table 9), while not correlated with NAO and AMO (not shown in Tables or Figures). The centroid locations for P, ET and Q are negatively correlated with ENSO, that is, the centroids for P, ET and Q move toward the south (north) during El Nino (La Nina) years. This can be further explained by the impacts of ENSO on P, ET and Q. Annual P and Q for the eastern U.S. is larger in positive ENSO years (6 and 20%, respectively) than in negative ENSO years (Figure 7). As discussed in the last section, the increase (decrease) in P, ET and Q during El Nino (La Nina) years is concentrated in the South Atlantic-Gulf region, which causes the centers of mass for P, ET and Q over eastern U.S. to move southward (northward). The difference of annual ET between positive and negative ENSO years is really small (0.4%) (Figure 7), which is because during positive ENSO years, the increased ET in the South-Atlantic region is offset by the decreased ET in Mid-Atlantic region (Figure 5). However, the opposite responses of ET to ENSO in Mid- and South-Atlantic regions lead to significant relation between ENSO and the centroid of ET. From Figure 7, we can find that the median centroids for P, ET, and Q are located 240, 140, and 40 km, respectively, more southward during El Nino years compared to those in La Nina years. From Figure 6, we can find that the centroid locations of P, ET, and Q move to the south by about 21, 5, and 46 km, respectively, when annual average ENSO index increases by 0.1. In contrast, the centroids of P, ET, and Q have a northward trend of roughly 3.3, 1.5, and 11.6 km/yr. This implies that both climate change and ENSO condition have impacts on the center of mass of freshwater export from the eastern U.S., and the northward trend in the freshwater centroid location likely induced by climate change may be disturbed by ENSO conditions. Similar to ENSO but to a less degree, the PDO also shows significant correlation with the centroid location of Q, which can be explained by the positive PDO-Q correlation in the South Atlantic-Gulf region.

TABLE 8. Trend in the Annual Centroid Location of Precipitation (P), Evapotranspiration (ET), and Streamflow (Q) from Gauged Watersheds Located along the Eastern United States for Water Years 1980-2014; Bold *p*-Values Indicate a Significant Trend at 5% Level of Significance.

	Spearman		**Mann-Kendall**	
	rho	***p***	**tau**	***p***
Q	0.302	0.078	0.203	0.086
P	0.255	0.140	0.173	0.144
ET	0.429	**0.010**	0.284	**0.016**

TABLE 9. Correlation with El Nino-Southern Oscillation (ENSO) and Pacific Decadal Oscillation (PDO) for the Annual Centroid Location of Precipitation (P), Evapotranspiration (ET), and Streamflow (Q) from Gauged Watersheds Located along the Eastern United States for Water Years 1980-2014; Bold *p*-Values Indicate a Significant Trend at 5% Level of Significance.

	ENSO				**PDO**			
	Spearman		**Mann-Kendall**		**Spearman**		**Kendall**	
	rho	***p***	**tau**	***p***	**rho**	***p***	**tau**	***p***
Q	−0.523	**0.001**	−0.348	**0.003**	−0.384	**0.023**	−0.272	**0.021**
P	−0.545	**0.001**	−0.382	**0.001**	−0.221	0.201	−0.148	0.211
ET	−0.497	**0.002**	−0.335	**0.005**	−0.416	**0.013**	−0.293	**0.013**

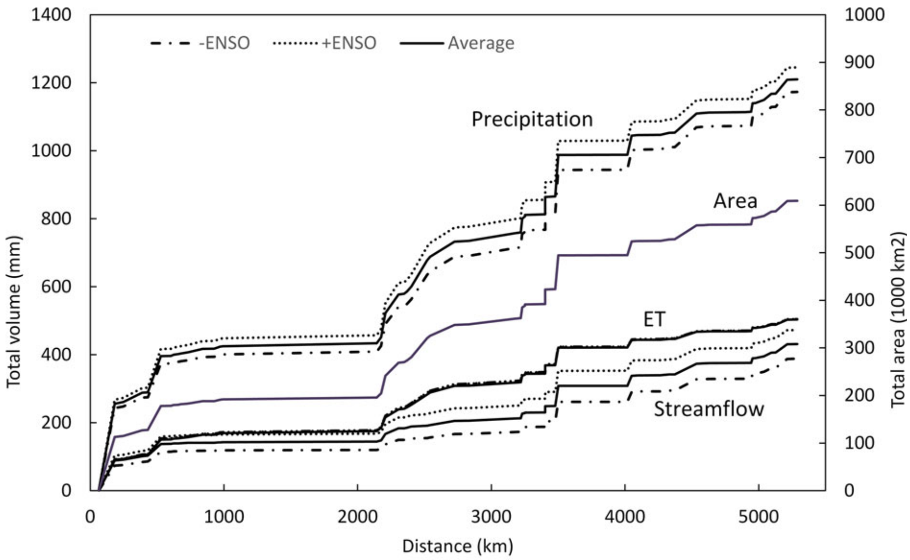

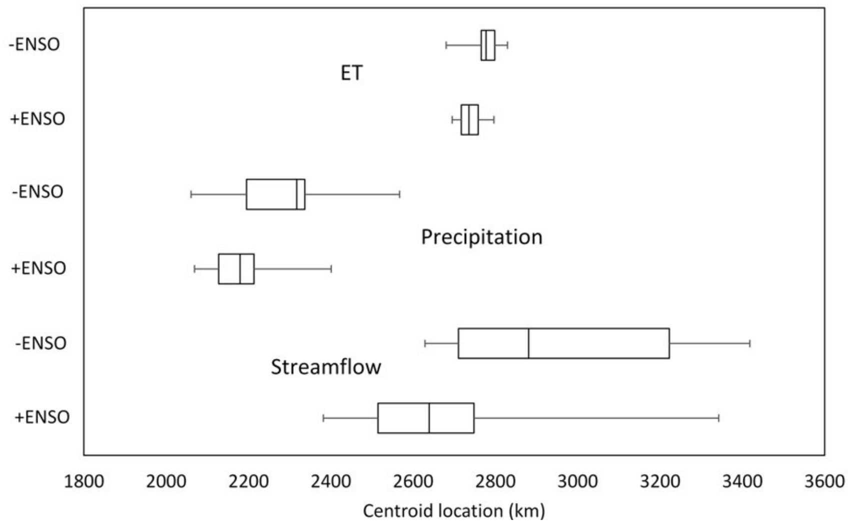

FIGURE 7. Annual Precipitation (P), Evapotranspiration (ET), and Streamflow (Q), and Drainage Area (Area) Accumulated from Gauged Watersheds along Eastern United States for Positive El Nino-Southern Oscillation (ENSO) Years (dash dot), Negative ENSO Years (dot), and All Years (solid) during Water Years 1980-2014 (top); Centroid Locations of Annual Precipitation (P), Evapotranspiration (ET), and Streamflow (Q) Integrated from Gauged Watersheds along Coastline for El Nino Years and La Nina Years during Water Years 1980-2014 (bottom).

The results found in this work suggest that if the global warming continues in the future, the center of annual freshwater mass over eastern U.S. would possibly move northward without significant change in total volume, especially in non-El Nino years. The changes in ENSO condition, especially the extreme El Nino events can disturb the northward trend. The results in this article combined with predictions of magnitude in global warming and ENSO extremes based on global climate models can be used to predict the inter-annual variability in Q over eastern U.S. For example, Cai *et al.* (2014) predicted that the frequency of extreme El-Nino events may double in the future; if this happens, the center of freshwater mass would move to the south more frequently than in the past. Considering the sediment and nutrients transported by the runoff, the spatial pattern as well as its relation to the climate factors found in this article can make some contribution to understanding the linkage between coastal ecosystem conditions and the climate factors in the background of global warming. However, it is important to note that the centroid assessment method presented here can mask east-west spatial variability (e.g., coastal *vs.* inland or Appalachians/Piedmont precipitation). Although not discussed here, there are east-west (coastal-inland) patterns in P and ET, that may be impacted by climate change and variability for which the centroid approach is not well suited to monitor.

CONCLUSIONS

An analysis on temporal and spatial variations in freshwater export from the eastern U.S. and corresponding linkages to climatic factors is presented for the period 1980-2014 (water years). Considering current global warming patterns and natural climate variability, we find that the streamflow variability in the northeast can be explained by climate change, and the intensified hydro-meteorological processes tended to increase streamflow in the northeast during the 1980-2014 period. The effects of climate change on streamflow can also be masked by internal climate variability. Here, we find the variability in streamflow in South Atlantic-Gulf region can be explained by the climate variabilities induced by conditions over Pacific Ocean. The increasing trend in Q from the northeast region results in a northward trend in the center of mass of Q. However, this trend can be disturbed by ENSO conditions, i.e., the centroid location of Q moves southward (northward) during El Nino (La Nina) years. The findings in this article suggest that the inter-annual variability in streamflow in the eastern U.S. is impacted by both climate change and internal climate fluctuations, especially the oceanic condition over the Pacific Ocean (i.e., ENSO and PDO), during the last 35 years. This finding may be useful for enhancing the predictability of streamflow and investigating ecosystem changes in relation to climate change (i.e., warmer conditions) in the eastern U.S. For example, these results may help explain observed variability on coastal ecosystems located along the eastern U.S.

Even though streamflow variations can be explained by climatic factors (i.e., similar patterns for P and Q), there are larger regions showing significant temporal trends or correlation with ENSO in Q as compared to P. This highlights the importance of understanding nonlinear rainfall-runoff processes (i.e., a small increase in P can result in a disproportionately larger increase in Q). Further work examining the effects of human activities (including land cover changes and water resources policies) on streamflow variation in this study region should also be performed. To extend the results of this study, future research investigating water quality measured along the eastern U.S. coastline (e.g., salinity, temperature, nutrients) could be performed to test if the terrestrial export patterns found here translate to observable coastal patterns, which could ultimately impact coastal ecosystems or water resources management.

ACKNOWLEDGMENTS

This research was funded by Northeastern University's Interdisciplinary Research Program and NASA's Terrestrial Hydrology Program (grant no. NNX12AQ36G and NNX14AD82G).

LITERATURE CITED

Alexander, M.A., I. Bladé, M. Newman, J.R. Lanzante, N.-C. Lau, and J.D. Scott, 2002. The Atmospheric Bridge: The Influence of ENSO Teleconnections on Air-Sea Interaction over the Global Oceans. Journal of Climate 15(16):2205-2231, DOI: 10.1175/1520-0442(2002) 015<2205:TABTIO>2.0.CO;2.

Barnett, T.P., J.C. Adam, and D.P. Lettenmaier, 2005. Potential Impacts of a Warming Climate on Water Availability in Snow-Dominated Regions. Nature 438(7066):303-309.

Baron, J., E. Hall, B. Nolan, J. Finlay, E. Bernhardt, J. Harrison, F. Chan, and E. Boyer, 2013. The Interactive Effects of Excess Reactive Nitrogen and Climate Change on Aquatic Ecosystems and Water Resources of the United States. Biogeochemistry 114 (1-3):71-92.

Barros, A., Y. Duan, J. Brun, and Medina M. Jr., 2014. Flood Nonstationarity in the Southeast and Mid-Atlantic Regions of the United States. Journal of Hydrologic Engineering 19 (10):05014014, DOI: 10.1061/(ASCE)HE.1943-5584.0000955.

Beighley, R. and G. Moglen, 2002. Trend Assessment in Rainfall-Runoff Behavior in Urbanizing Watersheds. Journal of Hydrologic Engineering 7(1):27-34, DOI: 10.1061/(ASCE)1084-0699 (2002) 7:1(27).

Beighley, R.E., T. Dunne, and J.M. Melack, 2008. Impacts of Climate Variability and Land Use Alterations on Frequency Distributions of Terrestrial Runoff Loading to Coastal Waters in Southern California. Journal of the American Water Resources Association 44(1):62-74, DOI: 10.1111/j.1752-1688.2007.00138.x.

Beighley, R.E., K.G. Eggert, T. Dunne, Y. He, V. Gummadi, and K.L. Verdin, 2009. Simulating Hydrologic and Hydraulic Processes throughout the Amazon River Basin. Hydrological Processes 23(8):1221-1235, DOI: 10.1002/hyp.7252.

Beighley, R.E. and V. Gummadi, 2011. Developing Channel and Floodplain Dimensions with Limited Data: A Case Study in the Amazon Basin. Earth Surface Processes and Landforms 36 (8):1059-1071, DOI: 10.1002/esp.2132.

Beighley, R.E. and Y. He, 2009. Predicting Model Uncertainty at River Junctions Due to Drainage Network Structure. Journal of Hydrologic Engineering 14(5):499-507, DOI: 10.1061/(ASCE) HE.1943-5584.0000007.

Beighley, R.E., J.M. Melack, and T. Dunne, 2003. Impacts of California's Climatic Regimes and Coastal Land Use Change on Streamflow Characteristics. Journal of the American Water Resources Association 39(6):1419-1433, DOI: 10.1111/j.1752-1688.2003.tb04428.x.

Birsan, M.V., L. Zaharia, V. Chendes, and E. Branescu, 2014. Seasonal Trends in Romanian Streamflow. Hydrological Processes 28(15):4496-4505.

Brutsaert, W., 2006. Indications of Increasing Land Surface Evaporation during the Second Half of the 20th Century. Geophysical Research Letters 33(20):L20403, DOI: 10.1029/2006GL027532.

Brutsaert, W. and M.B. Parlange, 1998. Hydrologic Cycle Explains the Evaporation Paradox. Nature 396(6706):30.

Cai, W., S. Borlace, M. Lengaigne, P. van Rensch, M. Collins, G. Vecchi, A. Timmermann, A. Santoso, M.J. McPhaden, L. Wu, M.H. England, G. Wang, E. Guilyardi, and F.-F. Jin, 2014. Increasing Frequency of Extreme El Nino Events due to Greenhouse Warming. Nature Climate Change 4(2):111-116, DOI: 10.1038/nclimate2100.

Cayan, D.R., K.T. Redmond, and L.G. Riddle, 1999. ENSO and Hydrologic Extremes in the Western United States. Journal of Climate 12(9):2881-2893, DOI: 10.1175/1520-0442(1999)012<2881:EAHEIT>2.0.CO;2.

Chalmers, A.T., P.C. Van Metre, and E. Callender, 2007. The Chemical Response of Particle-Associated Contaminants in Aquatic Sediments to Urbanization in New England, U.S.A. Journal of Contaminant Hydrology 91(1-2):4-25, DOI: 10.1016/j.jconhyd.2006.08.007.

Coleman, J.S.M. and D. Budikova, 2013. Eastern U.S. Summer Streamflow during Extreme Phases of the North Atlantic Oscillation. Journal of Geophysical Research—Atmospheres 118:4181-4193, DOI: 10.1002/jgrd.50326.

Dai, A., 2013. The Influence of the Inter-Decadal Pacific Oscillation on US Precipitation during 1923-2010. Climate Dynamics 41(3-4):633-646.

Dittmer, K., 2013. Changing Streamflow on Columbia Basin Tribal Lands—Climate Change and Salmon. Climatic Change 120(3):627-641, DOI: 10.1007/s10584-013-0745-0.

El-Shaarawi, A.H., S.R. Esterby, and K.W. Kuntz, 1983. A Statistical Evaluation of Trends in the Water Quality of the Niagara River. Journal of Great Lakes Research 9(2):234-240, DOI: 10.1016/S0380-1330(83)71892-7.

Emanuel, K., 2005. Increasing Destructiveness of Tropical Cyclones over the Past 30 Years. Nature 436(7051):686-688, DOI: 10.1038/nature03906.

Emanuel, K., 2015. Effect of Upper-Ocean Evolution on Projected Trends in Tropical Cyclone Activity. Journal of Climate 28(20):8165-8170, DOI: 10.1175/JCLI-D-15-0401.1.

Enfield, D.B., A.M. Mestas-Nuñez, and P.J. Trimble, 2001. The Atlantic Multidecadal Oscillation and Its Relation to Rainfall and River Flows in the Continental U.S. Geophysical Research Letters 28(10):2077-2080, DOI: 10.1029/2000GL012745.

Ficklin, D.L., J.T. Maxwell, S.L. Letsinger, and H. Gholizadeh, 2015. A Climatic Deconstruction of Recent Drought Trends in the United States. Environmental Research Letters 10(4):044009.

Gocic, M. and S. Trajkovic, 2013. Analysis of Changes in Meteorological Variables Using Mann-Kendall and Sen's Slope Estimator Statistical Tests in Serbia. Global and Planetary Change 100:172-182, DOI: 10.1016/j.gloplacha.2012.10.014.

Groisman, P.Y., R.W. Knight, and T.R. Karl, 2001. Heavy Precipitation and High Streamflow in the Contiguous United States: Trends in the Twentieth Century. Bulletin of the American Meteorological Society 82(2):219-246, DOI: 10.1175/1520-0477(2001) 082<0219:HPAHSI>2.3.CO;2.

Helsel, D.R. and R.M. Hirsch, 1992. Statistical Methods in Water Resources. Elsevier, Amsterdam.

Hipel, K.W. and A.I. McLeod, 1994. Time Series Modelling of Water Resources and Environmental Systems. Elsevier, Amsterdam, ISBN: 0080870368.

Hirsch, R.M. and J.R. Slack, 1984. A Nonparametric Trend Test for Seasonal Data with Serial Dependence. Water Resources Research 20(6):727-732, DOI: 10.1029/WR020i006p00727.

Horton, R.M., V. Gornitz, D.A. Bader, A.C. Ruane, R. Goldberg, and C. Rosenzweig, 2011. Climate Hazard Assessment for Stakeholder Adaptation Planning in New York City. Journal of Applied Meteorology and Climatology 50(11):2247-2266, DOI: 10.1175/2011JAMC2521.1.

Hu, Q. and S. Feng, 2012. AMO- and ENSO-Driven Summertime Circulation and Precipitation Variations in North America. Journal of Climate 25(19):6477-6495, DOI: 10.1175/JCLI-D-11-00520.1.

Jones, J.A., I.F. Creed, K.L. Hatcher, R.J. Warren, M.B. Adams, M.H. Benson, E. Boose, W.A. Brown, J.L. Campbell, and A. Covich, 2012. Ecosystem Processes and Human Influences Regulate Streamflow Response to Climate Change at Long-Term Ecological Research Sites. BioScience 62(4):390-404.

Kahya, E. and S. Kalaycı, 2004. Trend Analysis of Streamflow in Turkey. Journal of Hydrology 289(1):128-144.

Karl, T.R. and R.W. Knight, 1998. Secular Trends of Precipitation Amount, Frequency, and Intensity in the United States. Bulletin of the American Meteorological Society 79(2):231-241.

Karl, T.R., J.M. Melillo, and T.C. Peterson, 2009. Global Climate Change Impacts in the United States. Cambridge University Press, New York, ISBN: 0521144078.

Kaushal, S.S., G.E. Likens, R.M. Utz, M.L. Pace, M. Grese, and M. Yepsen, 2013. Increased River Alkalinization in the Eastern U.S. Environmental Science & Technology 47(18):10302-10311, DOI: 10.1021/es401046s.

Kendall, M.G., 1975. Rank Correlation Methods. Griffin, London.

Kenyon, J. and G.C. Hegerl, 2008. Influence of Modes of Climate Variability on Global Temperature Extremes. Journal of Climate 21(15):3872-3889.

Khaliq, M.N., T.B.M.J. Ouarda, P. Gachon, L. Sushama, and A. St-Hilaire, 2009. Identification of Hydrological Trends in the Presence of Serial and Cross Correlations: A Review of Selected Methods and Their Application to Annual Flow Regimes of Canadian Rivers. Journal of Hydrology 368(1-4):117-130, DOI: 10.1016/j.jhydrol.2009.01.035.

Kimmerer, W., 2002. Effects of Freshwater Flow on Abundance of Estuarine Organisms: Physical Effects or Trophic Linkages? Marine Ecology Progress Series 243:39-55.

Klotzbach, P.J., 2006. Trends in Global Tropical Cyclone Activity over the Past Twenty Years (1986-2005). Geophysical Research Letters 33(10):L10805, DOI: 10.1029/2006GL025881.

Knutson, T.R., J.L. McBride, J. Chan, K. Emanuel, G. Holland, C. Landsea, I. Held, J.P. Kossin, A.K. Srivastava, and M. Sugi, 2010. Tropical Cyclones and Climate Change. Nature Geoscience 3:157-163, DOI: 10.1038/ngeo779.

Kunkel, K.E. and J.R. Angel, 1999. Relationship of ENSO to Snowfall and Related Cyclone Activity in the Contiguous United States. Journal of Geophysical Research: Atmospheres 104(D16):19425-19434, DOI: 10.1029/1999JD900010.

Landsea, C.W., B.A. Harper, K. Hoarau, and J.A. Knaff, 2006. Can We Detect Trends in Extreme Tropical Cyclones? Science 313(5786):452-454, DOI: 10.1126/science.1128448.

Larson, J., Y. Zhou, and R.W. Higgins, 2005. Characteristics of Landfalling Tropical Cyclones in the United States and Mexico: Climatology and Interannual Variability. Journal of Climate 18(8):1247-1262.

Lehmann, E.L., 1975. Nonparametrics: Statistical Methods Based on Ranks. Holden-Day, San Francisco, California.

Lehner, B., K. Verdin, and A. Jarvis, 2008. New Global Hydrography Derived from Spaceborne Elevation Data. Eos 89(10):93-94.

Li, L., W. Li, and A.P. Barros, 2013. Atmospheric Moisture Budget and Its Regulation of the Summer Precipitation Variability over the Southeastern United States. Climate Dynamics 41(3-4):613-631, DOI: 10.1007/s00382-013-1697-9.

Li, L., W. Li, and Y. Kushnir, 2012. Variation of the North Atlantic Subtropical High Western Ridge and Its Implication to Southeastern US Summer Precipitation. Climate Dynamics 39(6):1401-1412, DOI: 10.1007/s00382-011-1214-y.

Li, W., L. Li, R. Fu, Y. Deng, and H. Wang, 2011. Changes to the North Atlantic Subtropical High and Its Role in the Intensification of Summer Rainfall Variability in the Southeastern United

States. Journal of Climate 24(5):1499-1506, DOI: 10.1175/2010JCLI3829.1.
Lins, H.F. and J.R. Slack, 1999. Streamflow Trends in the United States. Geophysical Research Letters 26(2):227-230.
Mann, H.B., 1945. Nonparametric Tests against Trend. Econometrica 13(3):245-259, DOI: 10.2307/1907187.
McPhaden, M.J., S.E. Zebiak, and M.H. Glantz, 2006. ENSO as an Integrating Concept in Earth Science. Science 314(5806):1740-1745, DOI: 10.1126/science.1132588.
Milly, P.C.D., K.A. Dunne, and A.V. Vecchia, 2005. Global Pattern of Trends in Streamflow and Water Availability in a Changing Climate. Nature 438(7066):347-350.
Mitchell, K.E., D. Lohmann, P.R. Houser, E.F. Wood, J.C. Schaake, A. Robock, B.A. Cosgrove, J. Sheffield, Q. Duan, L. Luo, R.W. Higgins, R.T. Pinker, J.D. Tarpley, D.P. Lettenmaier, C.H. Marshall, J.K. Entin, M. Pan, W. Shi, V. Koren, J. Meng, B.H. Ramsay, and A.A. Bailey, 2004. The Multi-Institution North American Land Data Assimilation System (NLDAS): Utilizing Multiple GCIP Products and Partners in a Continental Distributed Hydrological Modeling System. Journal of Geophysical Research: Atmospheres 109(D7): D07S90, DOI: 10.1029/2003JD003823.
Moglen, G. and R. Beighley, 2000. Using GIS to Determine Extent of Gauged Streams in a Region. Journal of Hydrologic Engineering 5(2):190-196, DOI: 10.1061/(ASCE)1084-0699(2000) 5:2(190).
Newman, M., G.P. Compo, and M.A. Alexander, 2003. ENSO-Forced Variability of the Pacific Decadal Oscillation. Journal of Climate 16(23):3853-3857, DOI: 10.1175/1520-0442(2003)016<3853:EVOTPD>2.0.CO;2.
Ning, L. and R.S. Bradley, 2014. Winter Precipitation Variability and Corresponding Teleconnections over the Northeastern United States. Journal of Geophysical Research: Atmospheres 119(13):7931-7945, DOI: 10.1002/2014JD021591.
Ning, L. and R.S. Bradley, 2015. Influence of Eastern Pacific and Central Pacific El Niño Events on Winter Climate Extremes over the Eastern and Central United States. International Journal of Climatology, DOI: 10.1002/joc.4321.
Ortegren, J.T., A. Weatherall, and J.T. Maxwell, 2014. Subregionalization of Low-Frequency Summer Drought Variability in the Southeastern United States. The Professional Geographer 66(2):323-332, DOI: 10.1080/00330124.2013.787008.
Pavelsky, T.M., M.T. Durand, K.M. Andreadis, R.E. Beighley, R.C.D. Paiva, G.H. Allen, and Z.F. Miller, 2014. Assessing the Potential Global Extent of SWOT River Discharge Observations. Journal of Hydrology 519(Part B):1516-1525, DOI: 10.1016/j.jhydrol.2014.08.044.
Pederson, N., A.R. Bell, E.R. Cook, U. Lall, N. Devineni, R. Seager, K. Eggleston, and K.P. Vranes, 2013. Is an Epic Pluvial Masking the Water Insecurity of the Greater New York City Region? Journal of Climate 26(4):1339-1354, DOI: 10.1175/JCLI-D-11-00723.1.
Peterson, T.C., V.S. Golubev, and P.Y. Groisman, 1995. Evaporation Losing Its Strength. Nature 377(6551):687-688.
Poona, A.K. and H.V. Storch, 1995. Monte Carlo Experiments on the Effect of Serial Correlation on the Mann-Kendall-Test of Trends. Meteorologische Zeitschrift 4(2):82-85.
Poveda, G., A. Jaramillo, M.M. Gil, N. Quiceno, and R.I. Mantilla, 2001. Seasonally in ENSO-Related Precipitation, River Discharges, Soil Moisture, and Vegetation Index in Colombia. Water Resources Research 37(8):2169-2178.
Quiñones, R.A. and R.M. Montes, 2001. Relationship between Freshwater Input to the Coastal Zone and the Historical Landings of the Benthic/Demersal Fish Eleginops Maclovinus in Central-South Chile. Fisheries Oceanography 10(4):311-328, DOI: 10.1046/j.1365-2419.2001.00177.x.
Ramadan, H., R. Beighley, and A. Ramamurthy, 2012. Temperature and Precipitation Trends in Lebanon's Largest River: The Litani Basin. Journal of Water Resources Planning and Management 139(1):86-95, DOI: 10.1061/(ASCE)WR.1943-5452.0000238.
Schulte, J.A., R.G. Najjar, and M. Li, 2016. The Influence of Climate Modes on Streamflow in the Mid-Atlantic Region of the United States. Journal of Hydrology: Regional Studies 5:80-99, DOI: 10.1016/j.ejrh.2015.11.003.
Seager, R., N. Pederson, Y. Kushnir, J. Nakamura, and S. Jurburg, 2012. The 1960s Drought and the Subsequent Shift to a Wetter Climate in the Catskill Mountains Region of the New York City Watershed. Journal of Climate 25(19):6721-6742, DOI: 10.1175/JCLI-D-11-00518.1.
Shadmani, M., S. Marofi, and M. Roknian, 2012. Trend Analysis in Reference Evapotranspiration Using Mann-Kendall and Spearman's rho Tests in Arid Regions of Iran. Water Resources Management 26(1):211-224.
Sheffield, J., E.F. Wood, and M.L. Roderick, 2012. Little Change in Global Drought over the Past 60 Years. Nature 491(7424):435-438, DOI: 10.1038/nature11575.
Tao, H., M. Gemmer, Y. Bai, B. Su, and W. Mao, 2011. Trends of Streamflow in the Tarim River Basin during the Past 50 Years: Human Impact or Climate Change? Journal of Hydrology 400(1):1-9.
Thompson, P.R., G.T. Mitchum, C. Vonesch, and J. Li, 2013. Variability of Winter Storminess in the Eastern United States during the Twentieth Century from Tide Gauges. Journal of Climate 26(23):9713-9726, DOI: 10.1175/JCLI-D-12-00561.1.
Tootle, G.A. and T.C. Piechota, 2006. Relationships between Pacific and Atlantic Ocean Sea Surface Temperatures and U.S. Streamflow Variability. Water Resources Research 42(7): doi:10.1029/2005WR004184.
Tootle, G.A., T.C. Piechota, and A. Singh, 2005. Coupled Oceanic-Atmospheric Variability and US Streamflow. Water Resources Research 41(12).
Trenberth, K.E., 2011. Changes in Precipitation with Climate Change. Climate Research 47(1):123.
Vecchi, G.A., S. Fueglistaler, I.M. Held, T.R. Knutson, and M. Zhao, 2013. Impacts of Atmospheric Temperature Trends on Tropical Cyclone Activity. Journal of Climate 26(11):3877-3891, DOI: 10.1175/JCLI-D-12-00503.1.
Vicente-Serrano, S.M., J.I. López-Moreno, S. Beguería, J. Lorenzo-Lacruz, A. Sánchez-Lorenzo, J.M. García-Ruiz, C. Azorín-Molina, E. Morán-Tejeda, J. Revuelto, R.M. Trigo, F. Coelho, and F. Espejo, 2014. Evidence of Increasing Drought Severity Caused by Temperature Rise in Southern Europe. Environmental Research Letters 4(9):44001, DOI: 10.1088/1748-9326/9/4/044001.
Wang, D. and M. Hejazi, 2011. Quantifying the Relative Contribution of the Climate and Direct Human Impacts on Mean Annual Streamflow in the Contiguous United States. Water Resources Research 47(10): W00J12.
Wikner, J. and A. Andersson, 2012. Increased Freshwater Discharge Shifts the Trophic Balance in the Coastal Zone of the Northern Baltic Sea. Global Change Biology 18(8):2509-2519, DOI: 10.1111/j.1365-2486.2012.02718.x.
Wooldridge, S.A., S.W. Franks, and J.D. Kalma, 2001. Hydrological Implications of the Southern Oscillation: Variability of the Rainfall-Runoff Relationship. Hydrological Sciences Journal 46(1):73-88.
Wu, H., L.-K. Soh, A. Samal, and X.-H. Chen, 2008. Trend Analysis of Streamflow Drought Events in Nebraska. Water Resources Management 22(2):145-164.
Xia, Y., K. Mitchell, M. Ek, J. Sheffield, B. Cosgrove, E. Wood, L. Luo, C. Alonge, H. Wei, and J. Meng, 2012. Continental-Scale Water and Energy Flux Analysis and Validation for the North American Land Data Assimilation System Project Phase 2 (NLDAS-2): 1. Intercomparison and Application of Model Products. Journal of Geophysical Research: Atmospheres 117(D3), D03109.

Xue, Y., T.M. Smith, and R.W. Reynolds, 2003. Interdecadal Changes of 30-Yr SST Normals during 1871-2000. Journal of Climate 16(10):1601-1612, DOI: 10.1175/1520-0442(2003)016<1601:ICOYSN>2.0.CO;2.
Yang, Q., H. Tian, M.A.M. Friedrichs, M. Liu, X. Li, and J. Yang, 2015. Hydrological Responses to Climate and Land-Use Changes along the North American East Coast: A 110-Year Historical Reconstruction. Journal of the American Water Resources Association 51(1):47-67, DOI: 10.1111/jawr.12232.
Yu, J. and Y. Zou, 2013. The Enhanced Drying Effect of Central-Pacific El Nino on US Winter. Environmental Research Letters 8:014019.
Yue, S., P. Pilon, and G. Cavadias, 2002. Power of the Mann-Kendall and Spearman's rho Tests for Detecting Monotonic Trends in Hydrological Series. Journal of Hydrology 259(1-4):254-271, DOI: 10.1016/S0022-1694(01)00594-7.
Zhang, Q., C. Liu, C.-Y. Xu, Y. Xu, and T. Jiang, 2006. Observed Trends of Annual Maximum Water Level and Streamflow during Past 130 Years in the Yangtze River Basin, China. Journal of Hydrology 324(1):255-265.
Zhang, X., K.D. Harvey, W. Hogg, and T.R. Yuzyk, 2001. Trends in Canadian Streamflow. Water Resources Research 37(4):987-998.
Zuo, D., Z. Xu, W. Wu, J. Zhao, and F. Zhao, 2014. Identification of Streamflow Response to Climate Change and Human Activities in the Wei River Basin, China. Water Resources Management 28(3):833-851, DOI: 10.1007/s11269-014-0519-0.